ACS Catalysis

Letter

pubs.acs.org/acscatalysis

Light-Driven Water Oxidation with Metal Hexacyanometallate Heterogeneous Catalysts

Sara Goberna-Ferrón,[†,§,¶] Willinton Y. Hernández,[†,¶] Barbara Rodríguez-García,[†] and José Ramón Galán-Mascarós*[,†,‡]

[†]Institute of Chemical Research of Catalonia (ICIQ), Avnida Paisos Catalans 16, E-43007 Tarragona, Spain

[‡]Catalan Institution for Research and Advanced Studies (ICREA), Passeig Lluis Companys, 23, E-08010 Barcelona, Spain

Supporting Information

ABSTRACT: The catalytic activity of metal hexacyanometallates (Prussian blue-type coordination polymers) was tested in photoactivated water oxidation by $[Ru(2\text{-}2'\text{-bpy})_3]^{2+}$/persulfate system at pH close to neutrality. This screening shows that manganese and cobalt N-coordinated compounds are able to catalyze the oxygen evolution reaction. Mn hexacyanometalates show low activity. Co hexacyanometalates, in contrast, appear highly active and promote robust catalysis with excellent quantum yield (≤88%), even in acidic media. Our results indicate that these catalysts are viable candidates for a photoactivated water oxidation process as part of an artificial photosynthesis scheme.

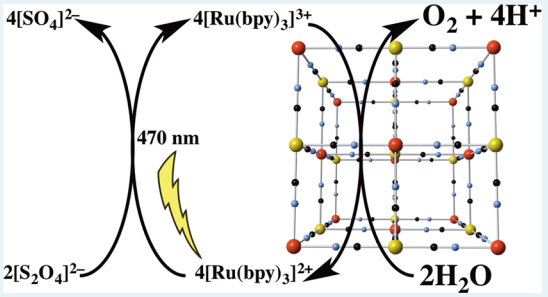

KEYWORDS: *artificial photosynthesis, cobalt, heterogeneous catalysis, Prussian blue, water oxidation*

The search for a fast, efficient, robust, and inexpensive catalyst that is able to promote water oxidation at low overpotential is one of the biggest challenges that chemists are facing today.[1−3] This arguably remains the essential "chemical problem" to be solved in the development of production of solar fuels.[4−6] Many research groups worldwide are currently studying plausible candidates, although few of them (if any) exhibit all the technological requirements.[7−20]

First-row transition metal oxides are currently leading this race,[21−27] particularly since Nocera et al. discovered that a cobalt oxide catalyst can function at neutral pH when stabilized by phosphate groups.[28−32] In general, the instability of metal oxides in ambient conditions is their biggest drawback. They work very well in basic media (pH > 13);[33] however, they are unstable at neutral pH and dissolve in acidic media, when the goal reaction, proton reduction, is thermodynamically easier to perform. In acid media, only noble metal oxides are currently good candidates, although this could be worked out with interesting novel strategies.[34]

Recently, we have discovered that modified electrodes with cobalt hexacyanoferrate thin films exhibit electrocatalytic water oxidation with competitive kinetics to those of metal oxides and unparalleled long-term stability in turnover conditions at neutral pH.[35] Herein, we explore the catalytic activity of Prussian blue (PB) analogues in a light-driven water oxidation reaction. These studies disclose the general requirements to find catalytic activity in these series and, more importantly, the excellent synergy of these PBs with chromophores for their subsequent application in a solar-powered water oxidation system.

Metal hexacyanometalates of general formula $A_{2x}M_{(3-x)}[M'(CN)_6]_2{\cdot}nH_2O$ (A = alkali metal) were synthesized as polycrystalline powders by the "drop by drop" method described by Berretoni et al.[36] All materials are characterized by the face-centered cubic structure (*Fm*-3*m* space group), typical of the PBs,[37−40] and an atomic ratio M/M′ close to 3:2 ($x \approx 0$, Supporting Information (SI) Figure S1 and Table S1). The structural and chemical properties observed correspond to the formation of lacunary type structures, where the $[M'(CN)_6]$ vacancies are filled by zeolitic and coordinated to the M cation water molecules. TGA confirmed the presence of ∼12−15 water molecules per unit formula on these compounds ((SI) Figure S2 and Table S1).

First, we studied the series M = Mn^{2+}, Fe^{2+}, Co^{2+}, Ni^{2+}, Cu^{2+}; M′ = Fe^{3+} (Mn−Fe, Fe−Fe, Co−Fe, Ni−Fe, and Cu−Fe, respectively), maintaining the $[Fe(CN)_6]^{3-}$ anion as the building unit while varying the N-coordinated cation. Coordination mode and oxidation states were confirmed by IR spectroscopy (Figure 1).

The most intense band corresponds to the principal ν(CN) vibration of the M−N≡C−Fe bridge, associated with the M^{n+} and Fe^{n+} oxidation state.[41] Table 1 lists the band position and its assignation according to literature reports.

Weak additional CN stretching bands are observed due to the nonstoichiometric nature of these compounds. These bands are related to possible linkage isomerization of the CN ligand (M−C≡N−M′ or M−N≡C−M′)[42] and to multiple oxidation states in the metal centers. All the synthesized materials showed a multielectron configuration, which implies the presence of a

Received: March 6, 2014
Revised: April 15, 2014
Published: April 16, 2014

   dx.doi.org/10.1021/cs500298e | ACS Catal. 2014, 4, 1637−1641

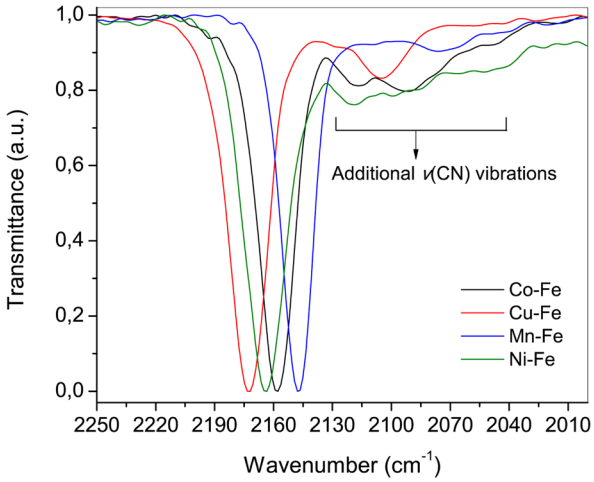

Figure 1. Enlarged and normalized IR spectra of ν(CN) region from the synthesized hexacyanoferrate complexes.

Table 1. Frequencies of CN Stretching, ν(CN), for the Synthesized Hexacyanoferrate Complexes

solid	band attribution	ν(CN) (cm^{-1})
Co−Fe	Fe^{III}−CN−Co^{II} (H.S.)	2158
	Fe^{II}−CN−Co^{III}	2117
	Fe^{II}−CN−Co^{II} (H.S.)	2091
Cu−Fe	Fe^{III}−CN−Cu^{II}	2172
	Fe^{II}−CN−Cu^{II}	2105
Mn−Fe	Fe^{III}−CN−Mn^{II} (H.S.)	2147
	Fe^{II}−CN−Mn^{II} (H.S.)	2066 (shoulder)
Ni−Fe	Fe^{III}−CN−Ni^{II}	2164
	Fe^{II}−CN−Ni^{II}	2099

minor content of partially reduced ferricyanide (to ferrocyanide), partially oxidized M^{2+} cations (to 3+), or both. Fe−Fe is a special case in which the main ν(CN) vibration, centered at 2052 cm^{-1}, shows a tail toward the lower wavenumber values (SI Figure S3) as a consequence of the fast and easy electron exchange in this mixed valence compound.[43]

Catalytic water oxidation, driven by a photosensitizer assay ($[Ru^{2+}(2-2'\text{-bpy})_3]$/persulfate), was evaluated in suspensions of these powders in a potassium phosphate buffer, pH 7.0. Oxygen evolution was monitored with a fluorescent probe for over 2.5 h upon illumination (Figure 2).

Co−Fe showed a fast and maintained oxygen production, whereas Mn−Fe showed weak but measurable activity. All other PBs were inactive. No oxygen evolution was observed upon light irradiation removing one of the key components of the photocalytic system: catalyst, $[Ru(bpy)_3]^{2+}$, or persultafe (SI Table S2). We estimated initial catalytic rates based on all the Co or Mn content in the bulk materials finding TOF = 3.0 × 10^{-4} s^{-1} and 2.2 × 10^{-5} s^{-1}, respectively.

Because the presence of cobalt in the hexacyanoferrate structure appears to be essential for having fast water oxidation catalysis, we studied three additional hexacyano complexes: M = Mn^{2+}, Fe^{2+}, and Co^{2+}; M′ = Co^{3+} (Mn−Co, Fe−Co, and Co−Co). The chemical and structural features of these materials are analogous to those established for the hexacyanoferrate series (SI Figure S4). Under the same experimental conditions, only Co−Co showed light-driven oxygen evolution activity (Figure 3). This indicates that Co^{3+} ions coordinated through the carbon end of the CN ligand

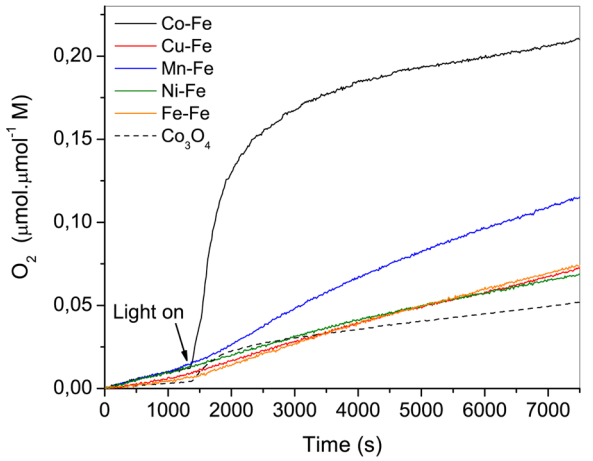

Figure 2. Catalytic oxygen evolution for the M−Fe series. Conditions: $[Ru(bpy)_3]^{2+}$ (1.0 mM), $Na_2S_2O_8$ (5.0 mM), and catalyst (10.0 mg) at pH 7.0. Light irradiation: 470 nm.

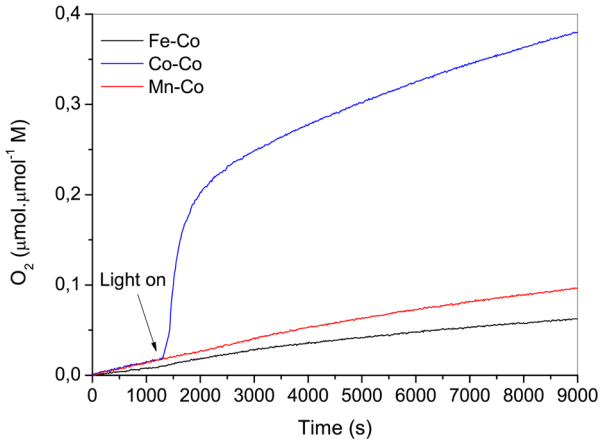

Figure 3. Catalytic oxygen evolution for the M-Co series. Conditions: $[Ru(bpy)_3]^{2+}$ (1.0 mM), $Na_2S_2O_8$ (5.0 mM), and catalyst (10.0 mg) at pH 7.0. Light irradiation: 470 nm.

($[Co(CN)_6]^{3+}$ units) are not participating in the catalytic process, probably because of the high chemical stability of the Co^{3+} ions in a low-spin configuration.[44,45] The TOF calculated for the Co−Co catalyst was 5.3 × 10^{-4} s^{-1} per mol of Co^{2+} (N-coordinated).

The superior performance of Co−Co could be a consequence of the chemical stability of the $[Co(CN)_6]^{3+}$ units. In Co−Fe, the Co^{2+}−N≡C−Fe^{3+} bridge is prone to linkage isomerism, and CN flipping stabilizes low-spin Co^{3+}.[46] Indeed, the IR spectra of the Co−Fe (Figure 1) shows additional CN stretching bands indicating multiple electronic configuration around the CN ligand, including the Co^{n+}−C≡N coordination mode. In the case of Co−Co, there is no linkage isomerism. The IR spectrum is clean, with only two ν(CN) vibrations, the Co^{2+}−N≡C−Co^{3+} bridge (2172 cm^{-1}, SI Figure S4-b) and a small band at 2132 cm^{-1}, that can be assigned to the Co^{2+}−N≡C−Co^{2+} electronic configuration.[47] Even if CN flipping eventually occurs in turnover conditions, one would not expect chemical differences because one cobalt center will always remain preferentially in high-spin configuration (N-bonded).

To put these data into context, we can compare them with that of Co_3O_4 spinel (powder, Sigma-Aldrich, S_{BET} 25 m^2/g),

dx.doi.org/10.1021/cs500298e | ACS Catal. 2014, 4, 1637−1641

that yielded 4.2×10^{-5} s^{-1} in the same experimental conditions (Figure 1). This Co_3O_4 sample contains particle sizes at least 20 times larger than the nanostructure clusters, which showed higher TOF values (from 2.12 to 4.05×10^{-4} s^{-1} per Co atom),[48−50] but even taking those into account, PB catalysts appear competitive with respect to state-of-the-art transition metal oxides.

Nonetheless, because only surface sites can be accessible to the $[Ru(bpy)_3]^{2+}$ complex during the catalytic process, the different surface-to-volume ratio and particle size could play an important role in these TOF estimations. Dynamic light scattering indicates that particle sizes are 208 ± 83 (Co−Fe) and 355 ± 88 nm (Co−Co) in the case of PBs, vs 627 ± 130 nm in the Co_3O_4 spinel samples (SI Figure S5). Thus, we have calculated the amount of surface-accessible cobalt active species in the respective catalyst structure from the BET surface area and crystal lattice parameters (see Supporting Information). Surface-normalized TOF values were 2.3×10^{-3}, 3.2×10^{-3}, and 2.6×10^{-3} s^{-1} per surface-accessible Co mol, for Co−Fe, Co−Co, and Co_3O_4, respectively. As observed, the reaction rate of Co−Co still remains the highest one among the analyzed materials.

One of the main issues in water oxidation catalysis is the possible transformation of a precatalyst into the corresponding oxide during the reaction. Because metal oxides are well known WOCs, it is important to gather additional data to rule out the significant participation of any adventitious oxide formed in situ. All experimental data and additional tests that we carried out support the genuine activity of the PB catalysts.

The catalytic activity of readily prepared or aged suspensions is identical upon light irradiation, which confirms that there is no evolution of the catalyst with time in the dark. We also carried out physicochemical characterization of the Fe−Co and Co−Co powders after the catalytic process (SI Figure S6 and S7). There are no significant differences in the X-ray powder diffraction patterns of the used catalysts with respect to the pristine materials, in either the position or shapes of the peaks, discarding any crystallinity loss or any decrease in particle size. Furthermore, there are significant changes in shape or metal content. Microanalysis also showed identical metal ratios and discards the presence of any Ru on the surface. Adventitious formation of cobalt oxide should occur by cobalt lixiviation from the respective cyano complexes, and some effect in the X-ray powder pattern, crystallinity, and metal content would be expected. Analogous IR spectra are also found regarding the CN region. Only the appearance of some additional IR bands between 1480 and 1270 cm^{-1} distinguishes the used materials. This can be attributed to the presence of the bpy ligand, which could bind surface metal centers.[51]

Raman spectroscopy and X-ray photoelectron spectroscopy (XPS) have been very useful for detection and characterization of the traces and nanostructures of cobalt oxide on surfaces.[52,53] The Raman spectra of the Co−Fe and Co−Co catalysts are typical of PB derivatives (SI Figure S8 and S9),[54] showing strong bands only in the cyanide region. After a catalytic cycle, the used catalysts show identical cyanide bands (SI Figure S10). The additional bands that appear in the Raman spectra of the used catalysts can be assigned almost exclusively to the presence of 2,2′-bpy on the surface (SI Figure S11 and S12).[55,56] Although bpy is a minority component, it exhibits surface-enhanced Raman scattering. Many and strong characteristic bpy Raman bands appear, including those expected for metal-bonding modes. This confirms that bpy is coordinating metal sites on the surface of the PB crystallites. A close examination of the low-energy region, where the cobalt oxide bands should appear (SI Figure S11 and S13), allows discarding the presence of cobalt oxide in the used catalysts. When compared with the experimental spectra obtained for Co_3O_4, none of the expected bands were found. Comparison and assignment of the Raman spectra bands is summarized in SI Table S3.

The XPS spectra of the catalysts before and after one water oxidation cycle do not show significant differences (SI Figures S14−S17 for the Co 2p, O 1s, Fe 2p, and N 1s XPS core levels, respectively), being clearly distinct from that of cobalt oxides.[57,58] In fact, the O 1s XPS spectra of the analyzed materials (SI Figure S15) clearly show that in the case of Co−Fe and Co−Co catalysts (freshly prepared and after one catalytic cycle), only peaks related to the presence of oxygen coming from water can be identified; that is, ≈534 eV for noncoordinated water and ≈532 eV for coordinated water.[59] The absence of lattice oxygen coming from cobalt oxide-type structures (around 530 eV) on the used catalysts is clear evidence of the lack of formation of cobalt oxides nanostructures during the catalytic process. Thus, Raman and XPS results confirm the status of Co−Fe and Co−Co materials as genuine water oxidation catalysts. It is worth mentioning that the XPS spectra of the used catalysts support the absence of Ru on the surface. No absorption peak corresponding to the Ru 3p core level was found.

We also performed an "acid test", by driving the light-induced water oxidation at pH ∼ 2.5 (SI Figure S8). PB catalysts are still able to promote light-induced oxygen evolution in these conditions, even when the overpotential available in the $[Ru(bpy)_3]^{2+/3+}$ redox pair is significantly low. The behavior of Co_3O_4 or $Co^{2+}(aq)$ species is completely different (SI Figure S8). The solution containing $Co^{2+}(aq)$ shows oxygen evolution in the dark, indicating that Co^{2+}, a well-known WOC in acid media,[60] is able to catalyze the direct oxidation of water by persulfate. In this experiment, oxygen evolution is continuous before light irradiation starts. Co_3O_4 shows analogous behavior, although at a slower pace. This is probably related to the slow dissolution of the oxide. In both cases, light irradiation does not affect the O_2 evolution trend. On the contrary, PBs suspensions show no O_2 evolution in the dark, even with recycled samples after carrying out one oxygen evolution cycle at pH 7 (vide infra). All these data support that the participation of adventitious cobalt oxide can be ruled out and that PBs are genuine water oxidation catalysts.

The used PB catalysts are still active in a second cycle (Figure 4) after being filtered and washed with Milli-Q water under sonication. When suspended in a new solution, they promote oxygen evolution under light irradiation, although with lower $TOF_i = 1.8 \times 10^{-4}$ and 2.7×10^{-4} s^{-1} for Co−Fe and Co−Co, respectively. In addition, a shift−time is observed. As already mentioned, the IR and Raman spectra of the used catalysts indicate the presence of bpy ligands coming from decomposition of the chromophore. Thus, bpy binding of the cobalt active sites should be at the origin of the decrease in catalytic activity. The 3:2 stoichiometry of these series of PBs, without significant content of alkali cations, yields an average of two water molecules bound to each Co^{2+} center, which could be substituted using bpy during the water oxidation process. Both catalysts show almost identical effect, losing ≈60% of their initial reaction rate (first to second cycle), and presenting the same shift time for starting the oxygen production (∼300 s

dx.doi.org/10.1021/cs500298e | ACS Catal. 2014, 4, 1637−1641

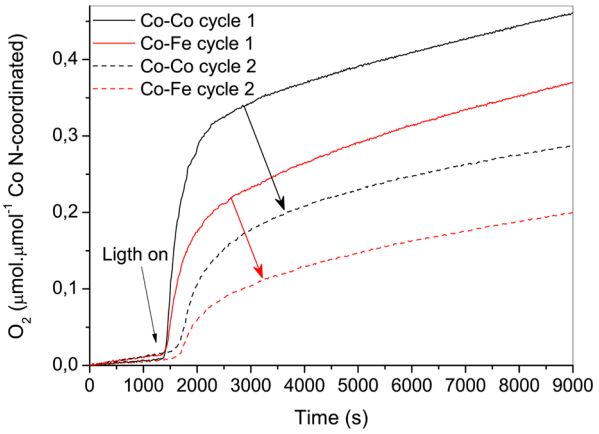

Figure 4. Oxygen evolution profiles as a function of the reaction cycles obtained for Co−Fe and Co−Co catalysts. Conditions: $[Ru(bpy)_3]^{2+}$ (2.0 mM), $Na_2S_2O_8$ (7.5 mM), and catalyst (10.0 mg) at pH 7.0. Light irradiation: 470 nm.

respect to the first cycle). This bpy poisoning increases during this second cycle. Barely any activity was found when the catalysts were used for a third time. Although undesired, this poisoning is an additional indirect proof that our PB catalysts are the genuine catalytic species, since this bpy poisoning has not been observed for any metal oxide.

An additional series of experiments was performed to determine the optimal sensitizer and persulfate concentrations by fixing the PB catalyst weight at 10 mg (SI Table S2) at neutral pH. These experiments show that the initial rate for oxygen production depends mostly on the Ru/Co ratio. The larger the ratio, the larger the number of PB crystals that receive a hole from a sensitizer. We achieved maximum initial TOFs of 4.5×10^{-4} and 8.1×10^{-4} s^{-1} for Co−Fe and Co−Co, respectively (expressed per total mol of Co N-coordinated). This corresponds to a maximum quantum yield of 52% for Co−Fe and 88% for Co−Co (during the first 5 min of illumination), assuming that the sensitizer absorbed all the photons (calculation details in the Supporting Information). This quantum yield is limited by the consumption of persulfate and decomposition of the chromophore.

In summary, the present catalyst screening confirms the activity and versatility of metal hexacyanometallate coordination polymers as heterogeneous water oxidation catalysts. Our results demonstrate that these PB derivatives promote catalytic water oxidation under light irradiation, with a blue light absorber and a sacrificial electron acceptor. Several experimental processes, including Raman, XPS, and water oxidation in acid media, support the genuine catalytic activity of these PBs, ruling out the participation of adventitious CoO_x species.

We found catalytic activity in the PBs containing Mn^{2+} or Co^{2+} coordinated through the N-end of the cyanide ligand. Among them, the all-cobalt PB exhibited the highest activity, exceeding the catalytic rates of classic metal oxides under these conditions, taking into account total surface area. Furthermore, Co−Co remains active in highly acidic media, and it is robust enough to run for at least two 3 h cycles. We have identified a deactivation process through surface poisoning by 2,2′-bipyridyl ligands, coming from chromophore decomposition, which block the active sites. This suggests that a bpy-free process should be desirable for further applications.

PB water oxidation catalysts appear as a viable alternative to metal oxides to promote water oxidation in artificial photosynthesis devices. They present competitive kinetics; better stability in neutral and acidic media; are obtained from Earth-abundant metals and materials; and can be easily processed as powders, thin-films, or nanoparticles[61−63] with classic coordination chemistry tools. Their catalytic activity as nanostructures is currently under study.

■ ASSOCIATED CONTENT

Ⓢ Supporting Information

Experimental details regarding synthesis, catalysis, and oxygen monitoring; structural and spectroscopic characterization data. This material is available free of charge via the Internet at http://pubs.acs.org.

■ AUTHOR INFORMATION

Corresponding Author

*E-mail: jrgalan@iciq.es.

Present Address

[§]Department of Chemistry and Center for Sustainable Materials Chemistry (CSMC), Oregon State University, Corvallis, Oregon 97331-4003, United States.

Author Contributions

[¶]S.G.-F. and W.Y.H. contributed equally.

Notes

The authors declare no competing financial interest.

■ ACKNOWLEDGMENTS

We are grateful for the financial support of the EU (ERC Stg Grant CHEMCOMP and COFUND 291787-ICIQ-IPMP), the Spanish Ministerio de Economía y Competitividad (Grant CTQ2012-34088), and the ICIQ Foundation. We thank F. Bozoglian and I. Martí from ICIQ Spectroscopy and Reaction Kinetics Unit, for their help in the collection and analysis of the Raman spectroscopy experiments.

■ REFERENCES

(1) Lewis, N. S.; Nocera, D. G. *Proc. Natl. Acad. Sci. U.S.A.* **2006**, *103*, 15729−15735.

(2) Karkas, M. D.; Johnson, E. V.; Verho, O.; Akermark, B. *Acc. Chem. Res.* **2013**, *47*, 100−111.

(3) Saleem, K.; Joya, Y. F.; Ocakoglu, K.; van de Krol, R. *Angew. Chem., Int. Ed.* **2013**, *52*, 10426−10437.

(4) Harriman, A. *Philos. Trans. R. Soc. A* **2013**, *371*, 20110415.

(5) Walter, M. G.; Warren, E. L.; McKone, J. R.; Boettcher, S. W.; Mi, Q.; Santori, E. A.; Lewis, N. S. *Chem. Rev.* **2010**, *110*, 6446−6473.

(6) Llobet, A.; Meyer, F. *Angew. Chem., Int. Ed.* **2011**, *50*, A30−A33.

(7) Concepcion, J. J.; Jurss, J. W.; Brennaman, M. K.; Hoertz, P. G.; Patrocinio, A. O. T.; Iha, N. Y. M.; Templeton, J. L.; Meyer, T. J. *Acc. Chem. Res.* **2009**, *42*, 1954−1965.

(8) Artero, V.; Fontecave, M. *Chem. Soc. Rev.* **2013**, *42*, 2338−2356.

(9) Sartorel, A.; Bonchio, M.; Campagna, S.; Scandola, F. *Chem. Soc. Rev.* **2013**, *42*, 2262−2280.

(10) Duan, L.; Bozoglian, F.; Mandal, S.; Stewart, B.; Privalov, T.; Llobet, A.; Sun, L. *Nat. Chem.* **2012**, *4*, 418−423.

(11) Lv, H.; Geletii, Y. V.; Zhao, C.; Vickers, J. W.; Zhu, G.; Luo, Z.; Song, J.; Lian, T.; Musaev, D. G.; Hill, C. L. *Chem. Soc. Rev.* **2012**, *41*, 7572−7589.

(12) Barnett, S. M.; Goldberg, K. I.; Mayer, J. M. *Nat. Chem.* **2012**, *4*, 498−502.

(13) Fillol, J. L.; Codola, Z.; Garcia-Bosch, I.; Gomez, L.; Pla, J. J.; Costas, M. *Nat. Chem.* **2011**, *3*, 807−813.

(14) Vickers, J. W.; Lv, H.; Sumliner, J. M.; Zhu, G.; Luo, G.; Musaev, D. G.; Geletii, Y. V.; Hill, C. L. *J. Am. Chem. Soc.* **2013**, *135*, 14110−14118.

(15) Spiccia, L.; Singh, A. *Coord. Chem. Rev.* **2013**, *257*, 2607−2622.
(16) Romain, S.; Vigara, L.; Llobet, A. *Acc. Chem. Res.* **2009**, *42*, 1944−1953.
(17) Dau, H.; Limberg, C.; Reier, T.; Risch, M.; Roggan, S.; Strasser, P. *ChemCatChem.* **2010**, *2*, 724−761.
(18) Evangelisti, F.; Güttinger, R.; Moré, R.; Luber, S.; Patzke, G. R. *J. Am. Chem. Soc.* **2013**, *135*, 18734−18737.
(19) Inoue, H.; Shimada, T.; Kou, Y.; Nabetani, Y.; Masui, D.; Takagi, S.; Tachibana, H. *ChemSusChem* **2011**, *4*, 173−179.
(20) Liu, X.; Wang, F. Y. *Coord. Chem. Rev.* **2012**, *256*, 1115−1136.
(21) Hocking, R. K.; Brimblecombe, R.; Chang, L.-Y.; Singh, A.; Cheah, M. H.; Glover, C.; Casey, W. H.; Spiccia, L. *Nat. Chem.* **2011**, *3*, 461−466.
(22) Minguzzi, A.; Fan, F.-R. F.; Vertova, A.; Rondinini, S.; Bard, A. J. *Chem. Sci.* **2012**, *3*, 217−229.
(23) Kent, C. A.; Concepcion, J. J.; Dares, C. J.; Torelli, D. A.; Rieth, A. J.; Miller, A. S.; Hoertz, P. G.; Meyer, T. J. *J. Am. Chem. Soc.* **2013**, *135*, 8432−8435.
(24) Sivula, K.; LeFormal, F.; Grätzel, M. *ChemSusChem* **2011**, *4*, 432−449.
(25) Suntivich, J.; May, K. J.; Gasteiger, H. A.; Goodenough, J. B.; Shao-Horn, Y. *Science* **2011**, *334*, 1383−1385.
(26) Maeda, K.; Ohno, T.; Domen, K. *Chem. Sci.* **2011**, *2*, 1362−1368.
(27) Smith, R. D. L.; Prevot, M. S.; Fagan, R. D.; Zhang, Z. P.; Sedach, P. A.; Siu, M. K. J.; Trudel, S.; Berlinguette, C. P. *Science* **2013**, *340*, 60−63.
(28) Kanan, M. W.; Nocera, D. G. *Science* **2008**, *321*, 1072−1075.
(29) Surendranath, Y.; Dinca, M.; Nocera, D. G. *J. Am. Chem. Soc.* **2009**, *131*, 2615−2620.
(30) Lutterman, D. A.; Surendranath, Y.; Nocera, D. G. *J. Am. Chem. Soc.* **2009**, *131*, 3838−3839.
(31) Surendranath, Y.; Kanan, M. W.; Nocera, D. G. *J. Am. Chem. Soc.* **2010**, *132*, 16501−16509.
(32) Surendranath, Y.; Lutterman, D. A.; Liu, Y.; Nocera, D. G. *J. Am. Chem. Soc.* **2012**, *134*, 6326−6336.
(33) McCrory, C. C. L.; Jung, S.; Peters, J. C.; Jaramillo, T. F. *J. Am. Chem. Soc.* **2013**, *135*, 16977−16987.
(34) Bloor, L. G.; Molina, P. I.; Symes, M. D.; Cronin, L. *J. Am. Chem. Soc.* **2014**, *136*, 3304−3311.
(35) Pintado, S.; Goberna-Ferrón, S.; Escudero-Adán, E. C.; Galán-Mascarós, J. R. *J. Am. Chem. Soc.* **2013**, *135*, 13270−13273.
(36) Berrettoni, M.; Giorgetti, M.; Zamponi, S.; Conti, P.; Ranganathan, D.; Zanotto, A.; Saladino, M. L.; Caponetti, E. *J. Phys. Chem. C* **2010**, *114*, 6401−6407.
(37) Ludi, A.; Gudel, H. U. *Struct. Bonding (Berlin)* **1973**, *14*, 1−21.
(38) Balmaseda, J.; Reguera, E.; Rodríguez-Hernández, J.; Reguera, L.; Autie, M. *Microporous Mesoporous Mater.* **2006**, *96*, 222−236.
(39) Widmann, A.; Kahlert, H.; Petrovic-Prelevic, I.; Wulff, H.; Yakhmi, J. V.; Bagkar, N.; Scholz, F. *Inorg. Chem.* **2002**, *41*, 5706−5715.
(40) Bhatt, P.; Yusuf, S. M.; Bhatt, R.; Schütz, G. *Appl. Phys. A* **2012**, *109*, 459−469.
(41) Sato, O.; Einaga, Y.; Fujishima, A.; Hashimoto, K. *Inorg. Chem.* **1999**, *38*, 4405−4412.
(42) Yusuf, S. M.; Thakur, N.; Kumar, A.; Yakhmi, J. V. *J. Appl. Phys.* **2010**, *107*, 053902.
(43) Ghosh, S. N. *J. Inorg. Nucl. Chem.* **1974**, *36*, 2465−2466.
(44) Nelson, K. J.; Miller, J. S. *Inorg. Chem.* **2008**, *47*, 2526−2533.
(45) Taube, H. *Chem. Rev.* **1952**, *50*, 69−126.
(46) Kumar, A.; Yusuf, S. M. *Phys. Rev. B* **2007**, *75*, 224419.
(47) Roque, J.; Reguera, E.; Balsameda, J.; Rodríguez-Hernández, J.; Reguera, L.; del Castillo, L. F. *Microporous Mesoporous Mater.* **2007**, *103*, 57−71.
(48) Jiao, F.; Frei, H. *Angew. Chem., Int. Ed.* **2009**, *48*, 1841−1844.
(49) Yusuf, S.; Jiao, F. *ACS Catal.* **2012**, *2*, 2753−2760.
(50) Rosen, J.; Hutchings, G. S.; Jiao, F. *J. Am. Chem. Soc.* **2013**, *135*, 4516−4521.
(51) Song, J.; Luo, Z.; Zhu, H.; Lian, T.; Kaledin, A. L.; Musaev, D. G.; Lense, S.; Hardcastle, K. I.; Hill, C. L. *Inorg, Chim. Acta* **2010**, *363*, 4381−4386.
(52) Ahn, H. S.; Yano, J.; Tilley, T. D. *Energy Environ. Sci.* **2013**, *6*, 3080−3087.
(53) Gallant, D.; Pezolet, M.; Simard, S. *J. Phys. Chem. B* **2006**, *110*, 687−6880.
(54) Clark, R. J. H.; Turtle, P. C.; Strommen, D. P.; Streusand, B.; Kincaid, J.; Nakamoto, K. *Inorg. Chem.* **1977**, *16*, 84−89.
(55) Alexander, B. D.; Dines, T. J.; Longhurst, R. W. *Chem. Phys.* **2008**, *352*, 19−27.
(56) Dines, T. J.; Peacock, R. D. *J. Chem. Soc., Faraday Trans.* **1988**, *84*, 3445−3457.
(57) Biesinger, M. C.; Payne, B. P.; Grosvenor, A. P.; Lau, L. W. M.; Gerson, A. R.; Smart, R.; St, C. *Appl. Surf. Sci.* **2011**, *257*, 2717−2730.
(58) La Rosa-Toro, A.; Berenguer, R.; Quijada, C.; Montilla, F.; Morallón, E.; Vázquez, J. L. *J. Phys. Chem. B* **2006**, *110*, 24021−24029.
(59) Kaplun, M. M.; Smirnov, Yu. E.; Mikli, V.; Malev, V. V. *Russ. J. Electrochem.* **2001**, *37*, 1065−1075.
(60) Gerken, J. B.; McAlpin, J. G.; Chen, J. Y. C.; Rigsby, M. L.; Casey, W. H.; Britt, R. D.; Stahl, S. S. *J. Am. Chem. Soc.* **2011**, *133*, 14431−14442.
(61) Talham, D. R.; Meisel, M. W. *Chem. Soc. Rev.* **2011**, *49*, 3356−3365.
(62) Catala, L.; Volatron, F.; Brinzei, D.; Mallah, T. *Inorg. Chem.* **2009**, *48*, 3360−3370.
(63) Clavel, G.; Larionova, J.; Guari, Y.; Guerin, C. *Chem.—Eur. J.* **2006**, *12*, 3798−3804.